Pergamon
www.elsevier.nl/locate/asr

Adv. Space Res. Vol. 23, No. 4, pp. 733–738, 1999

Printed in Great Britain
0273-1177/99 $20.00 + 0.00

PII: S0273-1177(99)00155-6

LUNAR ALBEDO FORCE MODELING AND ITS EFFECT ON LOW LUNAR ORBIT AND GRAVITY FIELD DETERMINATION

Rune Floberghagen[1], Pieter Visser[1] and Frank Weischede[2]

[1] *Delft Institute for Earth-Oriented Space Research (DEOS), Kluyverweg 1, 2629 HS, Delft, The Netherlands*
[2] *German Space Operations Center, Oberpfaffenhofen, Germany*

ABSTRACT

A force model for the lunar albedo effect on low lunar orbiters is developed on the basis of Clementine imagery and absolute albedo measurements. The model, named the *Delft Lunar Albedo Model 1* (DLAM-1), is a 15 × 15 spherical harmonics expansion, and is intended for improved force modeling for low satellite orbits as well as to minimise aliasing of non-gravitational force model defects in future lunar gravity solutions. The development of the model from the available lunar albedo data sources is described, followed by a discussion on its calibration using absolute albedo measurements and its correlation with main selenological features. DLAM-1 is next applied in low lunar orbit determination, and results for orbits typical of lunar mapping missions are presented. Finally, the effect of lunar albedo on future gravity solutions is analysed with particular emphasis on gravity mapping from global data sets, *i.e.* satellite-to-satellite tracking, which is expected to be a core experiment of coming lunar missions. It is shown that albedo-induced orbit perturbations have a magnitude and frequency signature which are non-negligible for precise orbit and gravity modeling. Radial orbit errors for low orbits are in the order of 1-2 m for one week arcs.

INTRODUCTION

The present-day quality of force models applicable to low lunar satellites does not allow highly precise determination of the orbits. Undoubtedly, the largely unknown gravitational potential of the Moon remains the most important perturbation force on low lunar satellites. It has, however, already been shown (Floberghagen *et al.*, 1996) that a global mapping of gravity by means of low-low satellite-to-satellite tracking (SST) is capable of bringing gravity-induced orbit errors down to levels acceptable for both selenodetic and remote-sensing orbits as well as lander operations. This paper therefore focuses on the effect of non-conservative forces, and in particular the yet unmodeled force due to the lunar albedo. As there is no atmosphere damping the backscattered solar radiation this force shows a strong peak near the sub-solar point. Moreover, the primary crust of the lunar highlands exhibits a high albedo in the order of 20-30%.

In detail the paper discusses the modeling aspects of the albedo radiation pressure and its influence on the orbit determination process. The albedo effect is modeled as a spherical harmonics series which may be evaluated for any point on the lunar surface. The force exerted on a spacecraft is computed by dividing the part of the lunar surface seen from the spacecraft into a number of rings and a polar cap, the rings being subdivided into concentric compartments or elements. The vector sum of the contributions from each compartment and the polar cap contains the total albedo force on the spacecraft. Albedo force computations are therefore more complex than conservative force computations, and may in cases like the Moon, where the geology (and hence reflectivity) exhibits strong spatial variations, require extensive computer time.

ALBEDO MODEL DEVELOPMENT

The primary data source for the albedo model development is a US Geological Survey (USGS) global albedo map derived from Clementine imagery. From roughly 50,000 images USGS has produced a mosaic of the Moon's albedo at a wavelength of 750 nm (USGS, 1996). This choice of wavelength corresponds to maximum reflectivity, and is just longward of the visible red. The main advantage of the USGS albedo map above Lunar Orbiter images, which are still the best in terms of spatial resolution, is the extensive far-side coverage. The global mosaicked image has

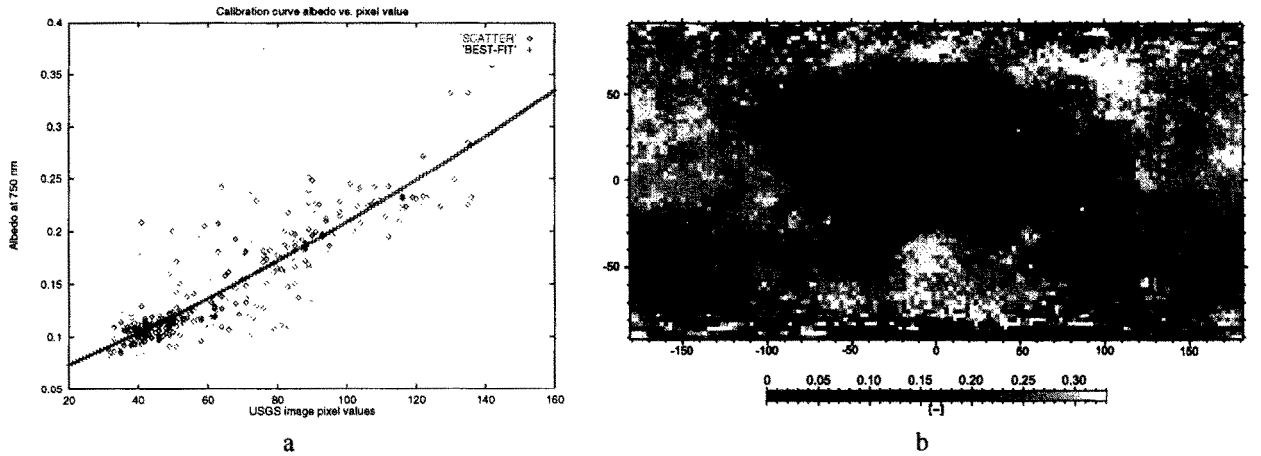

Figure 1. a. Calibration curve relating absolute albedo measurements, normalised to 750 nm wavelength to USGS global albedo image pixel values. b. Calibrated averaged, reduced-resolution global albedo image at 750 nm

a spatial resolution of 10 km/pixel, which enables the use of albedo data as a data source for first order geological studies and by far exceeds the needs of satellite force modeling. In deducing the global albedo USGS has used the pre-flight camera calibration data which does not correct fully for the brightness gradient across each frame, and this results in a small north-south striping of the global albedo image across the mosaic. This artifact is neglected in the further development of the DLAM-1. Moreover, the projection of the image is such that the albedo dominates the brightness everywhere, except near the poles, where topographic shading is significant. The global mapping of the lunar albedo at 750 nm enables the estimation of a spherical harmonics expansion of the lunar albedo a

$$a(\lambda,\phi) = \sum_{l=0}^{L} \sum_{m=0}^{l} \left[C_{lm} cos(m\lambda) + S_{lm} sin(m\lambda)\right] P_{lm}\left(sin(\phi)\right), \tag{1}$$

where λ and ϕ are the selenographical longitude and latitude of the evaluation point. L is the maximum degree and order of the expansion, C_{lm} and S_{lm} the harmonic coefficients and P_{lm} is the associated Legendre function, respectively. Eq. 1 may be evaluated at any location on the lunar surface and is therefore suitable for satellite force computations. Pixel values from the USGS albedo image were converted into albedo coefficients by means of a calibration curve, Figure 1a, estimated from available Earth-based absolute albedo observations. A total of 301 data points were found available for which spectral, photometric and polarimetric information can be derived (Vuorilehto and Korpela, 1994). These 301 albedo measurements are systematically distributed over the full near-side of the Moon. The calibration curve is a second order polynomial and fits to a root mean square (rms) value of 15.0%. Before estimation the albedo expansion, the USGS image was reduced to 75 × 75 km by block-averaging neighbouring pixels, Figure 1b. As can be seen from the calibrated, reduced-resolution image, extreme values for the lunar albedo occur for the polar areas, where topographic shading is pronounced. To avoid spurious effects in the spherical harmonics estimation, account was taken of the projection, and accordingly, high-latitude data was downweighted. DLAM-1 was finally estimated from the global albedo data by means of linear least-squares estimation, Figure 2. It was experimented with different expansion sizes for the model, where the main trade-off was between orbit computation time and a satisfactory representation of the major albedo features, but eventually it was settled for a 15 × 15 expansion. In terms of correlation with selenological features, DLAM-1 resolves all major near-side mare areas as well as the brighter highlands. However, DLAM-1 is limited by its size to surface features larger than a half-wavelength resolution of 12°, or approximately 360 km in diameter.

LUNAR ALBEDO FORCE MODELING

The standard reference paper for lunar albedo force modeling for satellites is Knocke *et al.* (1988). Basically, the part of the lunar sphere seen by the satellite is divided into a number of rings, and each ring is again subdivided into compartments or elements for each step along the satellite trajectory (integration step). The infinitesimal acceleration

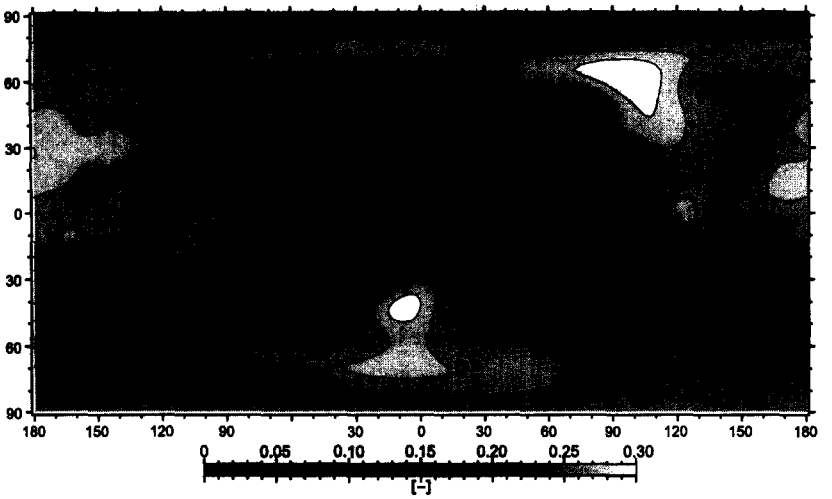

Figure 2. Delft Lunar Albedo Model 1 (DLAM-1)

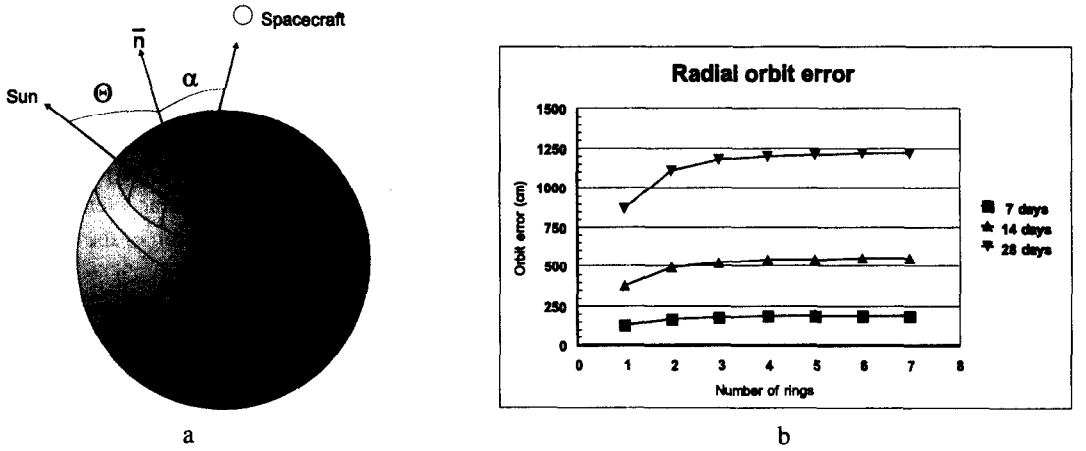

a b

Figure 3. a. The geometry of the lunar radiation pressure problem. b. Radial orbit errors for the Lunar Prospector orbit as a function of the number of rings and arc length.

vector $d\mathbf{a}$ induced by surface element i is given by

$$d\mathbf{a}_i = C_R\left(\tau a E_s cos\Theta_s + eM_B\right)\frac{A_c}{mc\pi r_i^2}cos\alpha\, dA\hat{\mathbf{r}}_i, \tag{2}$$

where C_R is the solar radiation pressure coefficient, τ the shadowing factor ($0 < \tau < 1$), a the albedo value from the spherical harmonics expansion, E_s the incident solar flux at the Moon, Θ_s the solar incidence angle at surface area element i, α the emission angle of area element, e the emissivity (not studied in this paper, hence $e = 0$), M_B the ideal black body thermal emission of the Moon, A_c the spacecraft cross-sectional area, m the spacecraft mass, c the speed of light, r the distance from the Moon surface element to the spacecraft, dA_i the area of lunar element i, r_i the distance of area of element i to the spacecraft and $\hat{\mathbf{r}}_i$ the unit vector from area of lunar element to the spacecraft. The geometry of the problem is depicted in Figure 3a.

IMPACT OF ALBEDO ON LOW LUNAR SATELLITE ORBITS

The first orbit test is the estimation of the required number of rings for an adequate and cost-effective modeling of the albedo force. In this analysis the s/c orbit itself is used as observable. Observability and tracking system performance are hence no issue. The test case is Lunar Prospector, orbiting at 100 km in a near-circular, 90° inclination orbit. The

Week no.	50 km alt.			100 km alt.		
	rad	alo	cro	rad	alo	cro
1	118	510	7	114	374	8
2	159	959	54	153	642	30
3	172	523	8	167	420	9
4	159	436	23	154	366	14
1+2	263	2475	37	253	1612	29
3+4	345	3301	72	329	1123	24
1+2+3+4	659	11020	330	617	6983	157

Table 1. RMS of orbit fit at 50 and 100 km altitude due to the lunar albedo using the actual satellite orbit as observable. The unit is cm.

s/c mass is 191.79 kg and the cross-sectional area is approximately 2 m^2. From Figure 3b it is concluded that the orbit errors show the expected asymptotic behaviour, and beyond 5 rings only marginal accuracy improvement is achieved. Hence, five rings is the chosen baseline for analysis using DLAM-1.

Spacecraft accelerations due to lunar albedo were next computed and were found to amount to about 20% of those induced by direct solar radiation, with peak amplitudes of about 10 nm/s^2. As opposed to the direct solar radiation pressure, for a spherically shaped body and a continuously sunlit orbit, the lunar albedo-induced force does not show a symmetric behaviour when viewed over one full orbital revolution. The dependence on surface material (rock) properties breaks the symmetry of the force applied to the satellite. Long-term effects on the satellite orbits coming from the non-symmetric reflectivity of the lunar rocks therefore accumulate in time. This forms the rationale for the inclusion of albedo in long-arc orbit studies. Also, it should be mentioned that albedo-induced accelerations are not exactly $\propto 1/r^2$ due to the fact that as the spacecraft orbit becomes higher, a slightly larger portion of the lunar surface becomes visible. In the range of low orbits, there is, hence, a small compensation mechanism.

Relatively long orbit arcs for selenodetic mapping purposes are the primary application of the model and naturally DLAM-1 has been implemented in the orbit determination (OD) process for such cases. Two different types of observables have been investigated, using GLGM-2 (Lemoine *et al.*, 1997) as priori gravity model:

- the satellite orbit itself
- a combination of Doppler and range tracking from Earth with low-low SST

Using the Orbit as Observable

Radial orbit errors (rms error w.r.t. orbits not perturbed by albedo) for arcs of 1, 2 and 4 weeks length are depicted Table 1. Inherent to the non-conservative nature of the force, the longer the arc, the larger the orbit error. Spectral analysis revealed that the larger portion of the orbit error is found at the low frequencies, primarily 0 to 2 cycles per revolution (cpr), with peaks near the resonant frequencies of 0 and 1 cpr. High-frequency orbit errors are only observable for very long arcs. For one week arcs, typical radial orbit errors range from 1 to 2 m. The along-track component is around 5 to 10 m. Going to, *e.g.*, one month arcs, radial errors increase to about 6 to 7 m and along-track errors to in the order of 100 m.

Using SST and Ground Tracking Observations

Future selenodetic missions are almost certain to conduct some sort of global mapping of the Moon's gravitational potential, cf. SELENE Project Team (1996). A mapping based on an inter-satellite tracking link seems the most likely method and a therefore test case where the satellite orbits are determined through low-low SST in combination with Earth-based ground tracking is also investigated. The inter-satellite angular separation is 3° in-plane (tandem), and

Week no.	50 km alt.			100 km alt.		
	rad	alo	cro	rad	alo	cro
1	118	1659	1568	113	1048	994
2	218	1091	152	196	736	103
3	193	3311	4161	176	2943	3735
4	178	593	1846	166	468	46

Table 2. RMS of orbit fit in cm for the chasing s/c in 50 and 100 km altitude low-low SST configurations due to lunar albedo. Note that the general trend of poor cross-track OD is due to the tandem orbit of the two s/c.

again orbit altitudes of 50 and 100 km are chosen. The main s/c (the chaser) is the active part of the SST configuration and is also tracked by two ESA ground stations (Madrid and Perth), applying a cut-off elevation of 20°. The target satellite in the SST is tracked solely by the chaser and its orbit determination is therefore through the SST Doppler measurements only. For the integrated SST Doppler measurements a sampling rate of 20 seconds is assumed with a precision of 0.1 mm/s. For the ground links 3m in range and 0.25 mm/s in Doppler are assumed. These values should be well within the reach of current or foreseen tracking systems.

The overall rms values for the orbit fits for one week arcs are shown in Table 2. Comparing with Table 1 one finds a slightly deteriorated determination of the along-track and cross-track components. For cross-track this is obviously due to the tandem nature of the two s/c orbits, which effectively implies that no cross-track information is available in the SST signal.Concerning the along-track component this is caused by the reduced observability of the very long-wavelength orbit perturbations by the short baseline SST experiment which inevitably reduces the along-track orbit quality. The general pattern of roughly 1-2 m perturbation in radial direction is nevertheless maintained.

ALBEDO-INDUCED ERRORS IN GRAVITATIONAL POTENTIAL MODELING

Estimating the impact of lunar albedo on gravity field solutions is slightly more complex. The main problem is the trade-off between arc length and the need for regularisation (constraining) of the solution. In general, if perfect non-linear equations can be set up, and a tracking complement gives perfect observability of the orbit perturbations, long arcs are to be preferred. For long arcs, however, the state-vector unknowns will correlate heavily with the gravitational potential coefficients, resulting in an unstable set of normal equations. In this case 2^{nd} order effects seriously degrade the gravity solution. The problem of observability may be counteracted by regularisation. This introduces, however, a bias in the gravity solution. In such cases, recovering the assumed-to-be true gravity model may be possible, but there will always remain an intrinsic contribution from the regularisation. Regularisation may furthermore smoothen albedo-induced features in the gravity field solution. As a consequence, in this paper the impact of albedo on the gravity modeling is shown for a limited number of cases only, and the role of regularisation is left for further study.

The gravitational potential is estimated up to degree and order 70 × 70 using GLGM-2 as a priori. Tables 3 and 4 show the RMS values for the errors, or difference in solution coming from the inclusion of albedo in the satellite force model, in selenoidal heights and gravity anomalies. For a mapping altitude of 100 km and combinations of one week arcs (2 or 4) the impact is found to be about 5 to 10 m in selenoidal height. Going down to 50 km altitude of the mapping orbit, it is seen that the increased observability of the orbit perturbations reduces this to about 2 m in selenoid heights and 5 to 10 mGal in gravity anomalies. As the prospected accuracy levels for a low-low SST mapping of gravity is around 2 mGal (Floberghagen *et al.*, 1996), it may be concluded that the introduction of DLAM-1 in the satellite force model will benefit the gravitational potential determination.

CONCLUSIONS

A 15^{th} degree and order spherical harmonics expansion called DLAM-1 for the lunar albedo as a function of selenographical location has been developed from a mosaic of 50,000 Clementine albedo images at a wavelength of 750 nm. The model has been successfully applied and assessed in both orbit determination and in gravity recovery simulations.

Week no.	50 km alt.		100 km alt.	
	ΔN	Δg	ΔN	Δg
1+2	3.11	17.42	9.26	52.42
3+4	1.77	9.86	8.20	47.55

Table 3. Global RMS value for selenoidal height errors induced by DLAM-1 using the satellite orbit as observable. The unit for selenoidal heights ΔN is m, for gravity anomalies Δg mGal.

Week no.	50 km alt.		100 km alt.	
	ΔN	Δg	ΔN	Δg
1+2	2.51	10.66	6.51	37.96
3+4	1.79	7.61	10.58	58.31
1+2+3+4	1.43	4.71	5.35	31.37

Table 4. Global RMS value for selenoidal height errors induced by DLAM-1 from a combination of SST and Earth-based Doppler and range tracking. Units as in Table 3.

Typical radial orbit errors at 100 km altitude are at the 1 to 2 m level for one week arcs, 3 m for two week arcs and up to 10 m for arcs of length one month. Such long arcs may be required for selenodetic mapping missions in order to have any substantial tracking data coverage of the lunar globe. In the spectral domain, the orbit errors are limited to the low frequency range, with the larger amplitudes between 0 and 4 cpr and also close to the resonant frequencies.

In terms of gravity, DLAM-1 is shown to have an effect above the accuracy threshold of prospective gravity solutions based on inter-satellite tracking. Typical error estimations are in the range of $\sim$ 5 to 10 mGal rms for global gravity anomalies and about 2 to 3 m in selenoid height.

Further work is anticipated on the inclusion of the thermal (infrared) part of the lunar radiation pressure, for which very little information is currently available.

ACKNOWLEDGEMENTS

The authors are grateful to Dr. Harald Hoffmann of DLR/Institut für Planetenerkundung, Berlin, Germany for supplying the absolute albedo measurements and bi-directional reflectance data for the calibration of DLAM-1. This work is partially funded and supported by Delft University of Technology's Center for High Performance Applied Computing (HPαC).

REFERENCES

Floberghagen, R., R. Noomen, P.N.A.M. Visser and G.D. Racca, Global Lunar Gravity Recovery From Satellite-to-satellite Tracking, *Plant. Space Sci.*, **44**(10), pp. 1081-1097 (1996).

Knocke, P.C., J.C. Ries and B.D. Tapley, Earth Radiation Pressure Effects on Satellites, AIAA-88- 4992-CP, in *Proc. of the AIAA/AAS Astrodynamics Conference*, pp. 577-586 (1988).

Lemoine, F., M. Zuber, G. Neumann and D. Rowlands, A 70^{th} degree lunar gravity model (GLGM-2) from Clementine and other tracking data, *J. Geophys. Res.*, **102**(E7), pp. 16339-16359 (1997).

SELENE Project Team, SELENE PROJECT (SELenological and Engineering Explorer), ISAS/NASDA Joint Moon Orbiting Satellite Project, *Project Folder* (1996).

USGS, Clementine web-site, http://wwwflag.wr.usgs.gov/USGSFlag/Space/clementine/clementine.html (1996).

Vuorilehto, A. and S. Korpela, Study of the Sun and the Moon as Radiation Calibration Targets, *Final Report, ESA Contract No. 10346/93/NL/CN* (1994).